Journal of the Serbian Society for Computational Mechanics / Vol. 12 / No. 1, 2018 / pp 108-125
(DOI: 10.24874/jsscm.2018.12.01.08)

Lie Group Analysis of Soret and Dufour Effects on Radiative Inclined Magnetic Pressure-Driven Flow Past a Darcy-forchheimer Medium

S.O. Salawu[1*], M.S. Dada[2]

[1]Department of Mathematics, Landmark University, Omu-aran, Nigeria
e-mail: kunlesalawu2@gmail.com
[2]Department of Mathematics, University of Ilorin, Ilorin, Nigeria.
**corresponding author*

Abstract

The study examines Soret and Dufour effects on steady convective heat and mass transfer of magnetohydrodynamic (MHD) pressure-driven flow in a Darcy-forchheimer porous medium with inclined uniform magnetic field and thermal radiation. The governing partial differential equations of the model are reduced to a system of coupled non-linear ordinary differential equations by applying a Lie group of transformations. The resulting coupled differential equations are solved using weighted residual method (WRM). The results obtained are presented graphically to illustrate the influence of various fluid parameters on the dimensionless velocity, pressure drop, temperature and concentration. Finally, the effects of Skin friction, Nusselt and Sherwood numbers results are presented and discussed accordingly.

Keyword: Soret; Dufour; radiation; Darcy-forchheimer; weighted residual method

1. Introduction

The study of the effects of Soret and Dufour on heat and mass transfer flow of an inclined magnetic field stimulated by the instantaneous actions of buoyancy forces consequential from mass and thermal diffusion with radiation in a non-Darcy permeable medium is significant from a practical as well as theoretical points of view due to their broad applications in planetary atmosphere research and others. In recent years, noticeably contribution has been made on the MHD flows as a result of its usefulness in devices such as hall accelerator, power engineering, MHD power generator and underground spreading of chemical wastes where the combined diffusion-thermo and thermal-diffusion effects are observed.

Due to its numerous applications, Umavathi, et al. (2010) considered heat transfer in a MHD Poiseuille-couette flow through an inclined channel using an analytical approach. Radiation and melting effects on flow over a vertical sheet in non-Darcy permeable media and non-Newtonian for opposing and supporting eternal fluid flows were verified by Ali et al. (2010). The result showed that the fluid momentum and heat raised with a rise in the non-Darcy parameter but in the case of aiding flow both the temperature and velocity distributions decreased with an increased in the values of non-Darcy parameter. In Abel and Monayya (2013), heat transfer flow of thermal slip or hydrodynamic past a linear stretching surface was examined. The above cited authors considered only heat transfer in the context of the fluid flow.

The symmetry transformation of heat and mass transfer are well known because its allows the transformation of the modelled partial differential equations into an ordinary differential equations. Follow from (Mansour et al. 2009; Sivasankaran et al. 2006), analysis of heat and mass transfer over an inclined plate invesitgated by applying Lie group method. The exact solution to the problem was obtained for the translational symmetry and it was reported that the velocity increased while heat and species fluid reduces with variational increased in the values of solutant and thermal Grashof parameters. In Dada and Salawu (2017); Mutlag et al. (2012), group transformation of radiative non-Newtonian flow fluid of heat transfer over a vertical moving surface with slip condition was analysed. Also, Reddy (2012) carried out analysis on temperature and species transfer of dissipative fluid flow along an inclined surface in the presence of heat generation by means of Lie group.

There is an improved interest in the study of MHD flow of heat and mass transfer past non-Darcy permeable medium as a result of its effect on the performance of systems and on boundary layer flow control using electrically conducting fluids. This kind of fluid flow is applicable in several engineering processes which includes nuclear reactors, geothermal energy extractions and many more. MHD heat and species transfer through a non-Darcy near drenched permeable medium was examined in (Seddeek et al. 2010; Vyas and Srivastava 2012; Salawu and Fatunmbi 2017; Kareem et al. 2018). It was found that a variational rise in the values of Prandtl number reduced the heat of the fluid while an increase in the porosity and Hartmann number decreased the velocity profiles because the magnetic force and the pores of the medium retarded the flow while Fenuga et al. 2018; Srinivasacharya and Reddy (2015) reported on the radiative and chemical reaction effects on heat and mass transfer in power-law flow through stretching surface in a permeable medium. In Kareem and Salawu (2017); Senapati et al. (2013), the effect of MHD on a chemical reaction Kuvshinski flow over a permeable medium in the existence of thermal radiation with constant heat and mass flux across moving plate was reported.

The heat flux can be created by both temperature and composition gradients. The created heat flux is referred to as Dufour while the created mass fluxes represent the Soret. These influences are considerable when density variations takes place in the flow system. The combine effects of Soret and Dufour are important in-between weighted molecular gases in fluid flow environment normally come across in engineering and chemical processes. As a result, Bazid et al. 2012; Bishwa and Animesh 2015) investigated the effects of heat Source, chemical reaction, Dufour and Soret by applying forchheimer model on heat and mass transfer flow entrenched in a permeable medium. It was observed that temperature and concentration was enhanced with a rise in Dufour and Soret parameter values. However, magnetic field, pressure gradient and the effect of radiation was neglected in the studied. Moreover, Srinivasacharya et al. (2015) studied the effects of Soret and Dufour on a vertical wavy surface with variable properties in a permeable medium.

Keeping the above studies in view, most of the researchers neglected the combined influences of Darcy-forchheimer porous medium, thermal-diffusion, diffusion-thermo and radiation on MHD flow. However, it is known that fluid physical properties can change significantly with thermal-diffusion and diffusion-thermo. Therefore, the present study examines the combined effects of Darcy-forchheimer permeable medium, inclined magnetic field, pressure drop, thermal radiation, Dufour and Soret on a steady convective heat and mass transfer of MHD flow.

2. Formulation of the problem

The convective heat and mass transfer of two dimensional magnetohydrodynamic pressure-driven fluid past a porous plate in Darcy-forchheimer permeable medium with radiation under the influence of uniform inclined magnetic field and pressure gradient. The fluid motion is maintained by both gravity and pressure gradient, and the flow is considered to be in the direction of X with Y-axis normal to it. Uniform magnetic field strength B_0 is introduced at angle α lying in the range $0 < \alpha < \frac{\pi}{2}$ in the fluid flow direction because of the interaction of the two fields, namely, velocity and magnetic fields, an electric field vector denoted E is induced at right angles to both V and B. This electric field is given by $E = V \times B$ while the density of the current induced in the conducting fluid denoted J is given by $J = \sigma E$ and simultaneously occurring with the induced current is the Lorentz force F given by $F = J \times B$. This force occurs because, as an electric generator, the conducting fluid cuts the lines of the magnetic field. The vector F is the vector cross product of both J and B and is a vector perpendicular to the plane of both J and B. This induced force is parallel to V but in opposite direction.

The Navier-Stokes equation is defined as:

$$\rho[(V \bullet V)]V = f_B - \nabla p + \mu \nabla^2 V \tag{1}$$

where ρ is the fluid density, $f_B = \sigma B_0^2 U$ is body force per unit mass of the fluid which define the magnetic force, μ is the fluid viscosity and p is the pressure acting on the fluid.

The geometry and equations governing the steady radiative heat and mass transfer of two-dimensional magnetohydrodynamics pressure-driven fluid flow in Darcy-forchheimer porous medium with inclined magnetic field are given below:

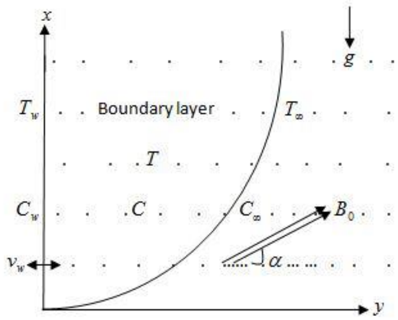

Fig. 1. The geometry of the model

Continuity equation

$$\frac{\partial U}{\partial X} + \frac{\partial V}{\partial Y} = 0 \tag{2}$$

Momentum equation in U-component

$$U\frac{\partial U}{\partial X}+V\frac{\partial U}{\partial Y}=-\frac{1}{\rho}\sigma B_0^2 Usin^2\alpha-\frac{1}{\rho}\frac{\partial P}{\partial X}+\nu\left(\frac{\partial^2 U}{\partial X^2}+\frac{\partial^2 U}{\partial Y^2}\right)-\frac{\nu}{K^*}U-\frac{b}{K^*}U^2+ \\ g\beta_T\left(T-T_\infty\right)+g\beta_C\left(C-C_\infty\right), \tag{3}$$

Momentum equation in V-component

$$U\frac{\partial V}{\partial X}+V\frac{\partial V}{\partial Y}=-\frac{1}{\rho}\frac{\partial P}{\partial Y}+\nu\left(\frac{\partial^2 V}{\partial X^2}+\frac{\partial^2 V}{\partial Y^2}\right), \tag{4}$$

Energy equation

$$\left(U\frac{\partial T}{\partial X}+V\frac{\partial T}{\partial Y}\right)=\frac{k}{\rho C_p}\left(\frac{\partial^2 T}{\partial X^2}+\frac{\partial^2 T}{\partial Y^2}\right)-\frac{1}{\rho C_p}\left(\frac{\partial q_X}{\partial X}+\frac{\partial q_Y}{\partial Y}\right)+ \\ \frac{DK_T}{C_s C_p}\left(\frac{\partial^2 C}{\partial X^2}+\frac{\partial^2 C}{\partial Y^2}\right)+\frac{Q_0}{\rho C_p}\left(T-T_\infty\right), \tag{5}$$

Concentration equation

$$U\frac{\partial C}{\partial X}+V\frac{\partial C}{\partial Y}=D\left(\frac{\partial^2 C}{\partial X^2}+\frac{\partial^2 C}{\partial Y^2}\right)+\frac{DK_T}{T_m}\left(\frac{\partial^2 T}{\partial X^2}+\frac{\partial^2 T}{\partial Y^2}\right)-\gamma\left(C-C_\infty\right), \tag{6}$$

The corresponding initial and boundary conditions are follows:

$$U=0, V=v_w, P=0, T=T_\infty+(T_w-T_\infty)AX, C=C_\infty+(C_w-C_\infty)BX \quad at \quad Y=0 \\ U=0, T=T_\infty, C=C_\infty \quad as \quad Y\to\infty \tag{7}$$

where U , V , P , C , and T are the velocity component in the X direction, velocity component in the Y direction, pressure, concentration of species in the fluid and temperature of the fluid respectively. A and B are constants defined as $A=B=\frac{1}{l}$, l is the characteristic length, B_0 is the magnetic field strength, α is the angle of inclination of the magnet, v_w is the permeability of the porous surface respectively. The physical quantities ν , b , K^* , ρ , σ , D, k , Q_0 and γ are the fluid kinematics viscosity, Forchheimer parameter, permeability of the porous medium, density, electric conductivity of the fluid, mass diffusion coefficient, thermal conductivity, rate of specific internal heat generation or absorption and reaction rate coefficient respectively. C_p , T_m , K_T , C_s , g are the specific heat at constant pressure, mean fluid temperature, thermal diffusion ratio, concentration susceptibility and gravitational acceleration respectively, while β_T and β_C are the thermal and concentration expansion coefficients respectively. q_X and q_Y are the radiative heat flux in the X and Y direction respectively. Using Rosseland diffusion approximation for radiation as in Reda (2013).

$$q_X = -\frac{4\sigma_0}{3\delta}\frac{\partial T^4}{\partial X} \quad and \quad q_Y = -\frac{4\sigma_0}{3\delta}\frac{\partial T^4}{\partial Y}, \tag{8}$$

where σ_0 and δ are the Stefan-Boltzmann and the mean absorption coefficient respectively. Assume the temperature difference within the flow are sufficiently small such that T^4 expressed as a linear function of temperature, using Taylor series to expand T^4 about the free stream T_∞ and neglecting higher order terms, gives the approximation

$$T^4 \cong 4T_\infty^3 T - 3T_\infty^4, \tag{9}$$

Using equation (8) and (9) leads to

$$\frac{\partial q_X}{\partial X} = -\frac{16\sigma_0 T_\infty^3}{3\delta}\frac{\partial^2 T}{\partial X^2} \quad \text{and} \quad \frac{\partial q_Y}{\partial Y} = -\frac{16\sigma_0 T_\infty^3}{3\delta}\frac{\partial^2 T}{\partial Y^2}, \tag{10}$$

Introducing the following non-dimensional quantities

$$x = \frac{X}{l}, y = \frac{Y}{l}, u = \frac{Ul}{v}, v = \frac{Vl}{v}, p = \frac{Pl^2}{\rho v^2}, \theta = \frac{T - T_\infty}{T_w - T_\infty}, \varphi = \frac{C - C_\infty}{C_w - C\infty}, \tag{11}$$

Substituting (10) and (11) into equation (2)-(7), to obtain

$$\frac{\partial u}{\partial x} + \frac{\partial v}{\partial y} = 0, \tag{12}$$

$$u\frac{\partial u}{\partial x} + v\frac{\partial u}{\partial y} = -H_a^2 sin^2\alpha u - \frac{\partial p}{\partial x} + \left(\frac{\partial^2 u}{\partial x^2} + \frac{\partial^2 u}{\partial y^2}\right) - D_a u - F_s u^2 + G_r\theta + G_c\varphi, \tag{13}$$

$$u\frac{\partial v}{\partial x} + v\frac{\partial v}{\partial y} = -\frac{\partial p}{\partial y} + \left(\frac{\partial^2 v}{\partial x^2} + \frac{\partial^2 v}{\partial y^2}\right), \tag{14}$$

$$u\frac{\partial \theta}{\partial x} + v\frac{\partial \theta}{\partial y} = \frac{1}{P_r}\left(1 + \frac{4}{3}R\right)\left(\frac{\partial^2 \theta}{\partial x^2} + \frac{\partial^2 \theta}{\partial y^2}\right) + D_u\left(\frac{\partial^2 \varphi}{\partial x^2} + \frac{\partial^2 \varphi}{\partial y^2}\right) + Q\theta, \tag{15}$$

$$u\frac{\partial \varphi}{\partial x} + v\frac{\partial \varphi}{\partial y} = \frac{1}{S_c}\left(\frac{\partial^2 \varphi}{\partial x^2} + \frac{\partial^2 \varphi}{\partial y^2}\right) + S_r\left(\frac{\partial^2 \theta}{\partial x^2} + \frac{\partial^2 \theta}{\partial y^2}\right) - \lambda\varphi, \tag{16}$$

The corresponding initial and boundary conditions are follows:

$$\begin{aligned} &u = 0, v = -f_w, p = 0, \theta = x, \varphi = x \quad at \quad y = 0 \\ &u = 0, \theta = 0, \varphi = 0 \quad as \quad y \to \infty, \end{aligned} \tag{17}$$

where $H_a = lB_0\sqrt{\dfrac{\sigma}{\mu}}$ is the Hartmann, $P_r = \dfrac{\mu C_p}{k}$ is the Prandtl, $S_c = \dfrac{\nu}{D}$ is the Schmidt, $G_r = \dfrac{l^3 g\beta_T\left(T_w - T_\infty\right)}{\nu^2}$ is the thermal Grashof, $G_c = \dfrac{l^3 g\beta_C\left(C_w - C_\infty\right)}{\nu^2}$ is the solutal Grashof, $\lambda = \dfrac{l^2\gamma}{\nu}$ is the concentration parameter, $Q = \dfrac{l^2 Q_0}{\mu C_p}$ is the heat source, $D_u = \dfrac{DKT(C_w - C_\infty)}{\nu C_s C_p (T_w - T_\infty)}$ is the Dufour, $S_r = \dfrac{DK_T (T_w - T_\infty)}{\nu T_m (C_w - C_\infty)}$ is the Soret, $f_w = -\dfrac{v_w l}{\nu}$ is the wall mass transfer coefficient, $R = \dfrac{4\sigma_0 T_\infty^3}{k\delta}$ is the Radiation parameter, $F_s = \dfrac{lb}{K^*}$ is the Forchheimer inertia term, $D_a = \dfrac{l^2}{K^*}$ is the Darcy parameter

Using the stream function $u = \dfrac{\partial\psi}{\partial y}$, $v = -\dfrac{\partial\psi}{\partial x}$ on equations (12) to (17), continuity equation is automatically. Also, introducing simplified form of Lie-group transformation on the equations, this is equivalent to determining the invariant solutions of these equations under a continuous one-parameter group Bhattacharyya et al. (2011). One of the methods is to search for a transformation group from an elementary set of one-parameter scaling group of transformations, given as ∇ such that

$$\begin{gathered}\nabla : x^* = xe^{\varepsilon\alpha_1}, y^* = ye^{\varepsilon\alpha_2}, \psi^* = \psi e^{\varepsilon\alpha_3}, u^* = ue^{\varepsilon\alpha_4}, v^* = ve^{\varepsilon\alpha_5}, \\ p^* = pe^{\varepsilon\alpha_6}, \theta^* = \theta e^{\varepsilon\alpha_7}, \varphi^* = \varphi e^{\varepsilon\alpha_8}\end{gathered} \tag{18}$$

where α_1, α_2, α_3, α_4, α_5, α_6, α_7, and α_8, are transformation parameters of the group to be determined later and ε is a small parameters. Equation (18) may be considered as a point-transformation which transforms coordinate $(x, y, \psi, u, v, \theta, \varphi)$ to the coordinate $(x^*, y^*, \psi^*, u^*, v^*, \theta^*, \varphi^*)$.

Substituting the transformation (18) into the equations and applying invariant conditions Pramanik (2013) to obtain the similarity transformations.

In order for the equations to stay unchanged under the transformations ∇, the subsequent relations exist between the parameters, that is

$$\alpha_3 = \alpha_4 = \alpha_7 = \alpha_8 = \alpha_1,\ \alpha_2 = \alpha_5 = \alpha_6 = 0 \tag{19}$$

Therefore, the set of transformations ∇ transforms to one parameter scaling group of transformations as

$$x^* = xe^{\varepsilon\alpha_1}\ y^* = y, \psi^* = \psi e^{\varepsilon\alpha_1}, u^* = ue^{\varepsilon\alpha_1}, v^* = v,\ p^* = p, \theta^* = \theta e^{\varepsilon\alpha_1}, \varphi^* = \varphi e^{\varepsilon\alpha_1} \tag{20}$$

Applying invariant conditions on equation (20) to obtain the similarity varables as follows

$$\eta = y, \psi = xf(\eta), p = p_d(\eta),..\theta = x\theta(\eta), \varphi = x\varphi(\eta) \tag{21}$$

Substituting the similarity variables (21) into the transformed equations to obtain the following system of non-linear differential equations:

$$f''' + ff'' - \left(1 + F_s\right) f'^2 - \left(H_a^2 sin^2\alpha + D_a\right) f' + G_r\theta + G_c\varphi = 0 \tag{22}$$

$$-p_d' = f'' + ff', \tag{23}$$

$$\left(1 + \frac{4}{3}R\right)\theta'' + D_u P_r \varphi'' + P_r f\theta' - P_r f'\theta + P_r Q\theta = 0 \tag{24}$$

$$\varphi'' + S_r S_c \theta'' + S_c f\varphi' - S_c f'\varphi - S_c \lambda\varphi = 0 \tag{25}$$

The corresponding initial and boundary conditions take the form:

$$\begin{aligned} &f = f_w, f' = 0, p_d = 0, \theta = 1, \varphi = 1 \ \ at \ \ \eta = 0 \\ &f' = 0, \theta = 0, \varphi = 0 \ \ as \ \ \eta \to \infty \end{aligned} \tag{26}$$

Integrating equation (23) with the initial and boundary conditions with $f_w = 1$, the pressure drop $G = -p_d$ becomes

$$G = f' + \frac{1}{2}f^2 - \frac{1}{2} \tag{27}$$

3. Method of solution

The idea of weighted residual method is to look for an approximate result, in the polynomial form to the differential equation given as

$$D\left[v(y)\right] = f \ \text{ in the domain } R,,\ A_\mu[v] = \gamma_\mu \ \text{ on } \partial R \tag{28}$$

where $D[v]$ represents a differential operator relating non-linear or linear spatial derivatives of the dependent variables v, f is the function of a known position, $A_\mu[v]$ denotes the approximate number of boundary conditions with R been the domain and ∂R the boundary. By assuming an approximation to the solution $v(y)$, an expression of the form

$$v(y) \approx w\left(y, a_1, a_2, a_3 ... a_n\right) \tag{29}$$

which depends on a number of parameters $a_1, a_2, a_3 ... a_n$ and is such that for arbitrary value a_i's the boundary conditions are satisfied and the residual in the differential equation become

$$E\left(y, a_i\right) = L\left(w\left(y, a_i\right)\right) - f\left(y\right) \tag{30}$$

The aim is to minimize the residual $E\left(y, a\right)$ to zero in some average sense over the domain. That is

$$\int_Y E\left(y, a\right) W_i dy = 0 \quad i = 1, 2, 3, ... n \tag{31}$$

where the number of weight functions W_i is exactly the same with the number of unknown constants a_i in w. Here, the weighted functions are chosen to be Dirac delta functions. That is, $W_i\left(y\right) = \delta\left(y - y_i\right)$, such that the error is zero at the chosen nodes y_i. That is, integration of equation (11) with $W_i\left(y\right) = \delta\left(y - y_i\right)$ results in $E\left(y, a_i\right) = 0$.

Weighted residual method (WRM) is applied to equations (22) to (27), by assuming the following trial polynomial functions with unknown coefficients to be determined.

$$f(\eta) = \sum_{i=0}^{n} a_i \eta^i, \theta(\eta) = \sum_{i=0}^{n} b_i \eta^i, \ \varphi(\eta) = \sum_{i=0}^{n} c_i \eta^i, \tag{32}$$

Imposing the boundary conditions (26) on the trial functions and substituting the functions into equations (22), (24) and (25), the residual is obtained and minimized to zero at some set of collocation points within the domain in order to obtain the unknown coefficients using Maple 2016 software.

Substituting the constant values into the trial functions to obtain the tangential velocity, temperature and concentration equations respectively.

$$\begin{aligned} f\left(\eta\right) &= 1.000000 + 1.717824\eta^2 - 2.295306\eta^3 + 1.799414\eta^4 - \\ &0.988332\eta^5 + 0.382705\eta^6 - 0.096954\eta^7 + 0.011625\eta^8 + \\ &0.001435\eta^9 - 0.000836\eta^{10} + 0.000133\eta^{11} - 0.0000084\eta^{12} \end{aligned} \tag{33}$$

$$\begin{aligned} \theta\left(\eta\right) &= 1.000000 - 0.516839\eta - 0.124909\eta^2 + 0.288289\eta^3 - \\ &0.252109\eta^4 + 0.165458\eta^5 - 0.084259\eta^6 + 0.032662\eta^7 - \\ &0.009402\eta^8 + 0.001941\eta^9 - 0.000271\eta^{10} + 0.000023\eta^{11} - 0.000008\eta^{12} \end{aligned} \tag{34}$$

$$\begin{aligned} \varphi\left(\eta\right) &= 1.000000 - 1.163307\eta + 0.595275\eta^2 - 0.013985\eta^3 - \\ &0.261476\eta^4 + 0.274318\eta^5 - 0.180803\eta^6 + 0.087308\eta^7 - \\ &0.031275\eta^8 + 0.008067\eta^9 - 0.001411\eta^{10} + 0.000149\eta^{11} - 0.000007\eta^{12} \end{aligned} \tag{35}$$

Differentiate equation (33) to obtain

$$f^{'}(\eta) = 3.435649\eta - 6.885905\eta^{2} + 7.197642\eta^{3} - 4.941652\eta^{4} + 2.296239\eta^{5} - 0.678626\eta^{6} + 0.092963\eta^{7} + 0.012832\eta^{8} - 0.008255^{9} + 0.001464\eta^{10} - 0.00010\eta^{11} \tag{36}$$

Also substituting for f and $f^{'}$ in (27) with the corresponding constant values to obtain the pressure drop as

$$\begin{aligned} G(\eta) = {} & -0.500000 + 3.435649\eta - 6.885905\eta^{2} + 7.197642\eta^{3} - \\ & 4.941652\eta^{4} + 2.296239\eta^{5} - 0.678626\eta^{6} + 0.092963\eta^{7} + \\ & 0.012832\eta^{8} - 0.008255\eta^{9} + 0.001464\eta^{10} - 0.000097\eta^{11} + \\ & \frac{1}{2}\Big(1.0000 + 1.727824562\eta^{2} - \\ & 2.295302\eta^{3} + 1.799411\eta^{4} - 0.988330\eta^{5} + 0.382707\eta^{6} \\ & -0.096946\eta^{7} + 0.011620\eta^{8} + \\ & 0.001426\eta^{9} - 0.000826\eta^{10} + 0.000133\eta^{11} - 0.000008^{12}\Big)^{2} \end{aligned} \tag{37}$$

The process of WRM is repeated for different values of the fluid parameters.

The physical quantity of practical interest are the local skin friction C_f, the Nusselt nuber N_u and the local sherwood number Sh defined as:

$$C_f = \frac{\tau_w}{\rho u_w^2}, \quad Nu = \frac{q_w x}{k(T_w - T_\infty)}, Sh = \frac{q_m x}{D(C_w - C_\infty)} \tag{38}$$

where k is the thermal conductivity of the fluid, τ_w, q_w and q_m are respectively given by

$$\tau_w = -\mu\left(\frac{\partial u}{\partial y}\right)_{y=0}, \quad q_w = -k\left(\frac{\partial T}{\partial y}\right)_{y=0}, \quad q_m = -D\left(\frac{\partial T}{\partial y}\right)_{y=0}, \tag{39}$$

Therefore, the local skin friction coefficient, local Nusselt number and local Sherwood number are

$$C_f Re_x^{\frac{1}{2}} = -f^{''}(0), \quad NuRe_x^{-\frac{1}{2}} = -\theta^{'}(0), ShRe_x^{-\frac{1}{2}} = -\varphi^{'}(0), \tag{40}$$

where $Re_x = \frac{u_w x}{\nu}$ is the local Reynolds number.

The following computational results in the table are obtained and compared with Runge-kutta method.

		Weighted Residual method			4^{th} order R-K		
PP	values	τ	Nu	Sh	τ	Nu	Sh
F_s	0.02	3.54343	0.52936	1.16808	3.54036	0.52937	1.16780
	1.0	3.43565	0.51684	1.16331	3.43595	0.51675	1.16288
	2.8	3.28520	0.49801	1.15644	3.28264	0.49775	1.15577
α	30^0	3.43565	0.51684	1.16331	3.43595	0.51675	1.16288
	40^0	3.03472	0.46523	1.14643	3.03210	0.46515	1.14591
	60^0	2.50106	0.39557	1.12452	2.49694	0.39421	1.12587
S_r	0.1	3.39251	0.48664	1.24440	3.39292	0.48657	1.24390
	1.0	3.43565	0.51684	1.16331	3.43595	0.51675	1.16288
	1.5	3.46443	0.53698	1.10451	3.46467	0.53688	1.10415
D_u	0.035	3.39350	0.68792	1.06136	3.39402	0.68770	1.06107
	0.5	3.43565	0.51684	1.16331	3.43595	0.51675	1.16288
	1.0	3.48804	0.27639	1.30592	3.48846	0.27658	1.30525

Table 1. Comparison of τ , Nu and Sh for various values of F_s , α , S_r , D_u and R

4. Results and discussion

The numerical analysis has been investigated for the velocity, temperature, concentration and pressure fields also skin friction coefficient, Nusselt and Sherwood numbers respectively at the plate have been examined for different values of the parameters. All graphs are corresponded to default values unless stated on appropriate graph.

Table 1 illustrates the effect of some physical parameters on skin friction, nusselt and sherwood number. It is clearly seen that an increase in the values of F_s and α decreases the skin friction while a rise in S_r and D_u increases skin friction. The temperature gradient decreases as the values of F_s , α and D_u increases except for S_r which decreases the temperature boundary layer and causes more heat to diffuse out of the system. Also, the numerical results show that the mass boundary layer increases as the values of D_u increases while F_s , α and S_r decrease mass gradient.

Figures 2 and 3 show the effect of the Hartmann number H_a on the velocity and pressure boundary layers thickness. Increasing H_a decreases the velocity and pressure distributions, since the magnetic field retarding flow as a result of lorentz force on the free convection fluid flow.

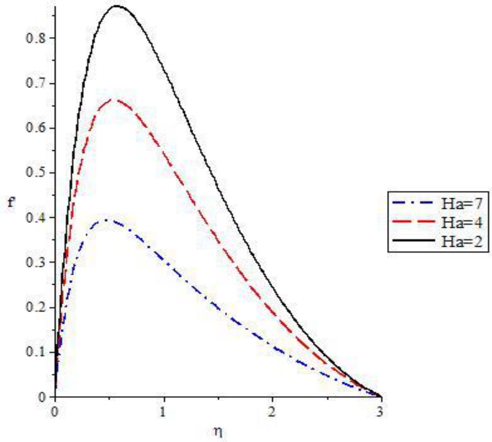

Fig. 2. Velocity profile for various values of *Ha*

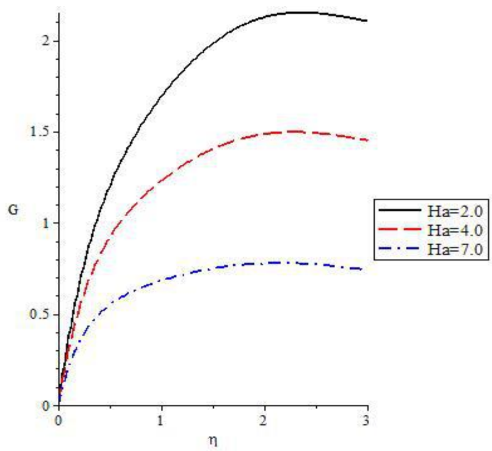

Fig. 3. Pressure profile for various values of *Ha*

Figures 4 and 5 bring out the effect of angles of inclination of the magnetic field α on the velocity and pressure profiles. An increase in the angle of inclination decreases the effect of the buoyancy forces and consequently the driving force to the flow decreases. Hence, velocity and pressure boundary layers thickness reduces that in turn decreases the velocity and pressure profile.

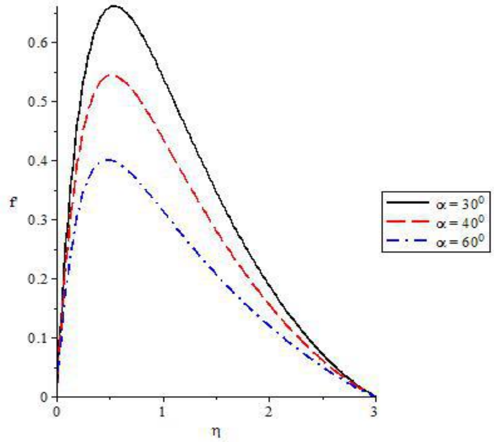

Fig. 4. Velocity profile for various l values of α

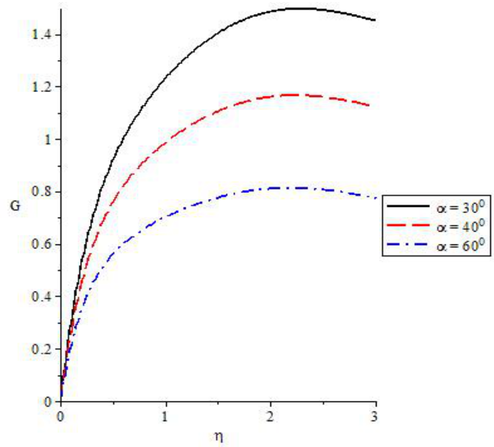

Fig. 5. Pressure profile for various values of α

Figures 6, 7, 8 and 9 show the effect of the inertial parameter F_s or porosity parameter D_a on the velocity and pressure profiles. It is observed that the velocity and pressure decreases as the porosity or inertial parameter increases. The reason for this behaviour is that the wall of the surface provides an additional resistance to the fluid flow mechanism, which causes the fluid to move at a retarded rate.

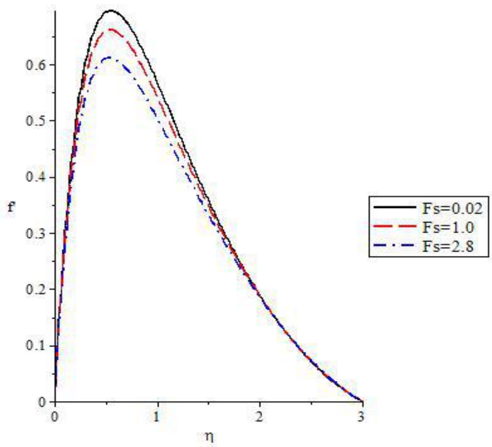

Fig. 6. Velocity profile for various values of F_s

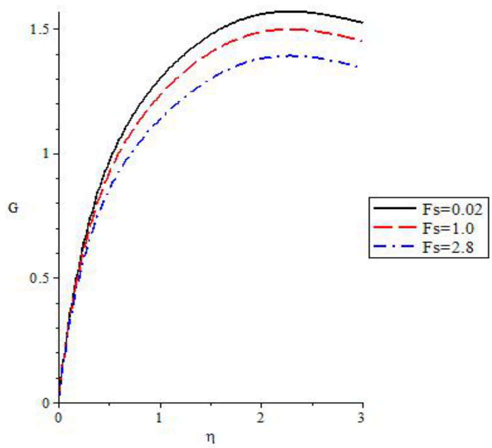

Fig. 7. Pressure profile for various al values of F_s

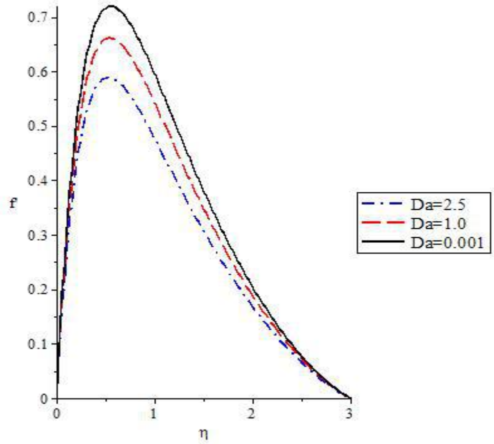

Fig. 8. Velocity profile for various values of D_a

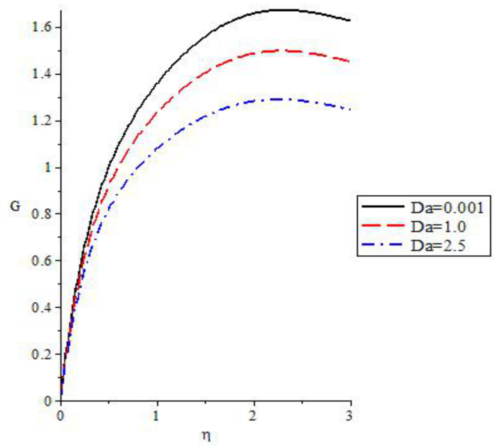

Fig. 9. Pressure profile for various values of D_a

Figure 10 show the influence of different values of the Prandtl number P_r on the temperature distribution. It is noticed that an increase in the ratio of momentum diffusivity to thermal diffusivity results in the respectively decrease temperature profile. This is because an increase in the P_r causes a decrease in the boundary layers thickness and decrease the average temperature within the boundary layers. Therefore, a rise in the Prandtl number increases the rate at which heat diffuse away from the heated surface to the environment.

The effect of Schmidt number S_c on the concentration profile are represented in Figure 11. Schmidt number is defined as the ratio of the momentum diffusivity to the mass diffusivity. An increase in S_c causes reduction in the concentration distribution which is accompanied by simultaneous decrease in the concentration boundary layer.

Figure 12 shows the variation in the thermal boundary layer with the Dufour number D_u. It is observed that the thermal boundary layers thickness increases with an increase in the Dufour number. While figure 13 depicts the variation in the mass transfer boundary layer with Soret number. It is found that the mass transfer boundary layers thickness increases with an increase in the Soret number.

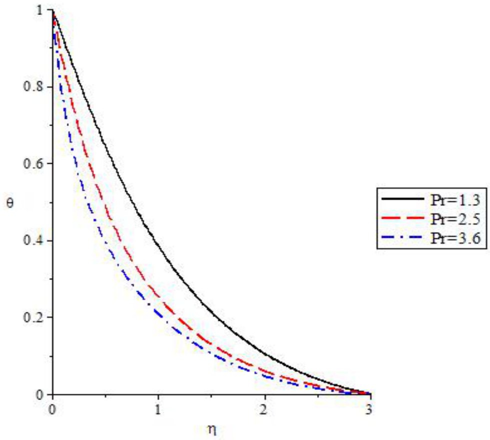

Fig. 10. Temperature profile for various values of P_r

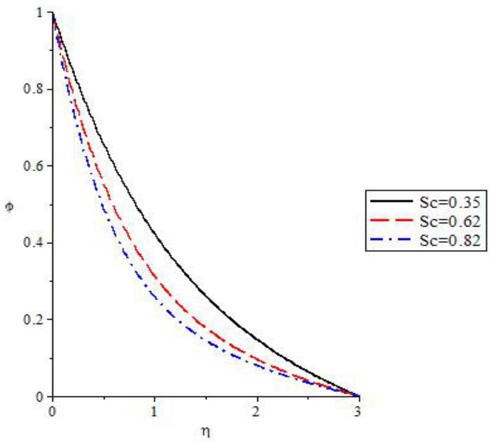

Fig. 11. Concentration profile for various values of S_c

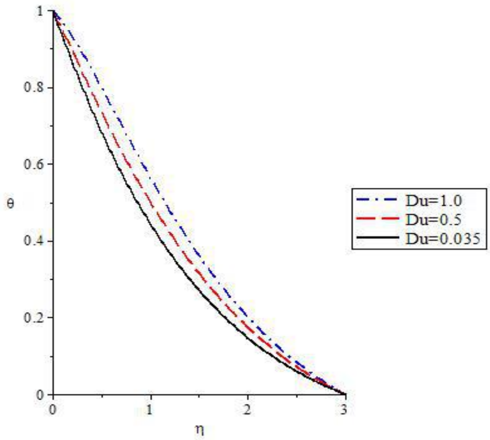

Fig. 12. Temperature profile for various values of D_u

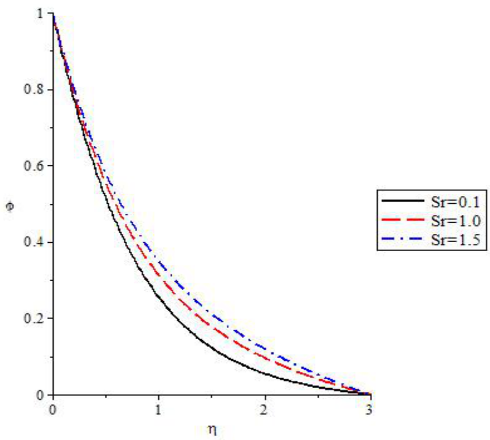

Fig. 13. Concentration profile for various values of S_r

5. Conclusion

The dimensionless form of the formulated governing equations are reduced to a couple ordinary differential equations by using a simplify form of Lie group transformation. The numerical solution is obtained using weighted residual method. From the numerical results, it is seen that an increase in the values of Hartmann, degree of inclination of the magnetic field, porosity parameter, inertial parameter, prandtl or schmidt numbers is exhibited as a decrease in the flow velocity, pressure, temperature or concentration distribution. The velocity, pressure, temperature or concentration profile increases as the Soret and Dufour increases respectively.

References

Abel MS and Monayya M (2013). MHD flow and heat transfer of the mixed hydrodynamic thermal slip over a linear vertically stretching sheet, International Journal of Mathematical Archive, 4(5): 156-163.

Ali JC, Sameh EA and Abdulkareem SA (2010). Melting and radiation effects on mixedconvection from a vertical surface embedded in a non-Newtonian fluid saturated non-Darcy porous medium for aiding and opposing eternal flows, International Journal of the Physical Sciences, 5(7): 1212-1224.

Bazid MAA, Gharsseldien ZM, Seddeek MA and Alharbi M (2012). Soret and Dufour numbers effect on heat and mass transfer in stagnation point flow towards a stretching surface in the presence of buoyancy force and variable thermal conductivity, Journal of Computations & Modelling, 2(4): 25-50.

Bhattacharyya K, Uddin MS and Layek GC (2011). Application of scaling group of transformations to steady boundary layer flow of Newtonian fluid over a stretching sheet in presence of chemical reactive species, Journal of Bangladesh Academy of Sciences, 35(1): 43-50.

Bishwa RS and Animesh A (2015). Influence of chemical reaction, heat source, Soret and Dufour effects on heat and mass transfer in boundary layer flow over a stretching cylinder embedded in a porous medium using Brinkman-Forchheimer extended Darcy model, International Journal of Innovative Research in Science, Engineering and Technology, 4(1): 18635-18644.

Dada MS, Salawu SO (2017). Analysis of heat and mass transfer of an inclined magnetic field pressure-driven flow past a permeable plate, Applications and Applied Mathematics: An International Journal (AAM), 12(1), 189 – 200.

Fenuga OJ, Abiala IO, Salawu SO (2018). Analysis of thermal boundary layer flow over a vertical plate with electrical conductivity and convective surface boundary conditions, Physical Science International Journal, 17(2), 1-9.

Kareem RA, Salawu SO, Gbadeyan JA (2018). Numerical analysis of non-uniform heat source/sink in a radiative micropolar variable electric conductivity fluid with dissipation Joule heating, American Journal of Applied Mathematics, 6(2), 34 – 41.

Kareem RA, Salawu SO (2017). Variable viscosity and thermal conductivity effect of Soret and Dufour on inclined magnetic field in non-Darcy permeable medium with dissipation, British Journal of Mathematics & Computer Science, 22(3): 1-12.

Mansour MA, Mohamed RA, Abd-Elaziz MM and Ahmed SE (2009). Lie group analysis of unsteady MHD mixed convection boundary layer flow of a micropolar fluid along a symmetric wedge with variable surface temperature saturated porous medium, Int. J. of Appl. Math and Mech, 5(2): 97-114.

Mutlag AA, Uddin Md J, Ismail AI Md and Hamad MAA (2012). Scaling group transformation under the effect of thermal radiation heat transfer of a non-Newtonian power-law fluid over a vertical stretching sheet with momentum slip boundary condition, Applied Mathematical Sciences, 6(121): 6035-6052.

Pramanik S (2013). Applications of scaling group of transformations to the boundary layer flow of a non-Newtonian power-law fluid. Int. journal of Appl. Math and Mech., 9(6),1-13.

Reddy MG (2012). Lie group analysis of heat and mass transfer effects on steady MHD free convection dissipative fluid flow past an inclined porous surface with heat generation, Theoret. Appl. Mech, 39(3): 233-254.

Reda GA (2013). MHD slip flow of newtonian fluid past a stretching sheet with thermal convective boundary condition, radiation, and chemical reaction, Hindawi Publishing Corporation Mathematical Problems in Engineering, 1-12.

Salawu SO, Fatunmbi EO (2017). Dissipative heat transfer of micropolar hydromagnetic variable electric conductivity fluid past inclined plate with Joule heating and non-uniform heat generation, Asian Journal of Physical and Chemical Sciences, 2(1), 1-10.

Seddeek MA, Akl MY and Al-Hanaya, AM (2010). Thermal radiation effect on mixed convection and mass transfer flow on vertical porous plate with heat generation and chemical reaction by using scaling group, Journal of Natural Sciences and Mathematics Qassim University, 4(1): 41-60.

Senapati N, Dhal RK and Ray K (2013). Effect of chemical reaction on MHD free convection on Kuvshinshki fluid through porous medium in presence of heat radiation with constant heat and mass flux across moving plate, International Journal of Applied Mathematics & Statistical Sciences, 2(4): 45-52.

Sivasankaran S, Bhuvaneswari M, Kandaswamy P and Ramasami EK (2006). Lie group analysis of natural convection heat and mass transfer in an inclined surface, Nonlinear Analysis Modelling and Control, 11(1): 201-212.

Srinivasacharya D, Mallikarjuna B and Bhuvanavijaya R (2015). Soret and Dufour effects on mixed convection along a vertical wavy surface in a porous medium with variable properties, Ain Shams Engineering Journal, 6(15): 553-564.

Srinivasacharya D and Reddy GS (2015). Chemical reaction and radiation effects on mixed convection heat and mass transfer over a vertical plate in power-law fluid saturated porous medium, Journal of the Egyptian Mathematical Society, 8(15): 1-8.

Umavathi JC, Liu IC and Kumar JP (2010). Magnetohydrodynamics Poiseuille couette flow and heat transfer in an inclined channel, Journal of Mechanics, 26(4): 525-532.

Vyas P and Srivastava N (2012). On dissipative radiative MHD boundary layer flow in a porous medium over a non isothermal stretching sheet, Journal of Applied Fluid Mechanics, 5(4): 23-31